Human Molecular Genetics, 2018, Vol. 27, No. 6 1078–1092

doi: 10.1093/hmg/ddy029
Advance Access Publication Date: 17 January 2018
Original Article

ORIGINAL ARTICLE

Analysis of the human SOX10 mutation Q377X in mice and its implications for genotype-phenotype correlation in SOX10-related human disease

Kathrin Truch[1], Juliane Arter[1], Tanja Turnescu[1], Matthias Weider[1], Anna C. Hartwig[1], Ernst R. Tamm[2], Elisabeth Sock[1] and Michael Wegner[1,*]

[1]Institut für Biochemie, Emil-Fischer-Zentrum, Friedrich-Alexander Universität Erlangen-Nürnberg, D-91054 Erlangen, Germany and [2]Institut für Humananatomie und Embryologie, Universität Regensburg, D-93053 Regensburg, Germany

*To whom correspondence should be addressed at: Institut für Biochemie, Emil-Fischer-Zentrum, Friedrich-Alexander Universität Erlangen-Nürnberg, Fahrstrasse 17, D-91054 Erlangen, Germany. Tel: +49 9131 85 24620; Fax: +49 9131 85 22484; Email: michael.wegner@fau.de

Abstract

Human SOX10 mutations lead to various diseases including Waardenburg syndrome, Hirschsprung disease, peripheral demyelinating neuropathy, central leukodystrophy, Kallmann syndrome and various combinations thereof. It has been postulated that PCWH as a combination of Waardenburg and Hirschsprung disease, peripheral neuropathy and central leukodystrophy is caused by heterozygous *SOX10* mutations that result in the presence of a dominantly acting mutant SOX10 protein in the patient. One such protein with postulated dominant action is SOX10 Q377X. In this study, we generated a mouse model, in which the corresponding mutation was introduced into the *Sox10* locus in such a way that Sox10 Q377X is constitutively expressed. Heterozygous mice carrying this mutation exhibited pigmentation and enteric nervous system defects similar to mice in which one *Sox10* allele was deleted. However, despite presence of the mutant protein in Schwann cells and oligodendrocytes throughout development and in the adult, we found no phenotypic evidence for neurological defects in peripheral or central nervous systems. In the nervous system, the mutant Sox10 protein did not act in a dominant fashion but rather behaved like a hypomorph with very limited residual function. Our results question a strict genotype-phenotype correlation for SOX10 mutations and argue for the influence of additional factors including genetic background.

Introduction

The transcription factor Sox10 is an important regulator in neural crest and central nervous system (CNS) in all vertebrates so that mutation or deletion of the *Sox10* gene lead to severe developmental disturbances (1). In humans, SOX10 mutations are usually sporadic and heterozygous. They may cause several diseases, including Waardenburg syndrome as a melanocyte defect, Hirschsprung disease as a defect of the enteric nervous system, peripheral demyelinating neuropathy as a Schwann cell defect, central dysmyelinating leukodystrophy as an oligodendrocyte defect, and Kallmann syndrome as a defect in olfactory ensheathing cells, that prevents migration of neurons from the olfactory placode into the CNS and thereby interferes with production of gonadotropin releasing hormone from these neurons in the hypothalamus (2–6). Frequently patients suffer from a combination of these defects. The most common syndrome observed is Waardenburg–Hirschsprung disease; the most dramatic is PCWH where Peripheral demyelinating neuropathy and Central dysmyelinating leukodystrophy are combined with

Received: August 15, 2017. **Revised:** January 12, 2018. **Accepted:** January 12, 2018

Waardenburg and Hirschsprung diseases. Corresponding Online Mendelian Inheritance in Man (OMIM) numbers are #609136, #611584 and #613266.

Depending on the severity of myelin defects in peripheral nervous system (PNS) and CNS, PCWH patients exhibit variable symptoms that often include delayed motor and cognitive development, cerebral palsy, ataxia, spasticity, congenital nystagmus, hyporeflexia, distal sensory impairments and distal muscle wasting.

Determinants of the exact disease phenotype are still not completely clear but include the genetic background. At least in the decision between isolated Waardenburg or Waardenburg–Hirschsprung disease the same mutation can give rise to both (7). Additionally, the exact type of SOX10 mutation appears to play a role (2, 8).

Numerous disease-causing missense, nonsense, frameshift and deletion mutations have been identified for *SOX10* (7). A comparison of the *SOX10* nonsense and frameshift mutations has led to the observation that mutations in the last exon are frequently associated with PCWH, whereas their occurrence in the preceding exons usually correlates with Waardenburg, Hirschsprung or Waardenburg–Hirschsprung diseases (2). In vitro experimental evidence argued that differential susceptibility of mutant transcripts to nonsense-mediated decay (NMD) may lie at the bottom of this phenomenon, as nonsense and frameshift mutations often escape NMD when localized in the last exon. The altered proteins generated from these transcripts may then exert a dominant function and cause PCWH. In all other cases, proteins may not be produced, resulting in haploinsufficiency and a milder disease phenotype such as Waardenburg, Hirschsprung or Waardenburg–Hirschsprung syndrome that is also observed following heterozygous *SOX10* deletion. Although differential NMD susceptibility of mutant transcripts represents an attractive hypothesis, there is little *in vivo* evidence so far.

In principle, such evidence may be obtained in model organisms as Sox10 function is highly conserved in vertebrates with homozygous loss or inactivation leading to developmental defects in oligodendrocytes of the CNS and several neural crest lineages including melanocytes, cells of the enteric nervous system and peripheral glia such as Schwann cells and olfactory ensheathing cells (9–14).

Recently, Ito *et al.* (15) generated a mouse model in which a PCWH-associated mutant SOX10 protein is produced from a BAC transgene. The underlying *SOX10* mutation (SOX10 c.1400del12) deletes 12 base pairs in the last exon at the end of the open reading frame including the stop codon and thereby extends translation into the 3′ UTR so that 82 amino acids are added to the carboxyterminus (16). With increasing number of transgene copies, animals exhibit a delay in the differentiation of Schwann cells and oligodendrocytes, and a hypomyelinating phenotype that is more prominent in the CNS than in the peripheral nerve (15). This study supports a causal link between the presence of the mutant SOX10 protein and the PCWH phenotype. However, the mutant SOX10 protein is special in that it carries additional amino acids, whereas most other mutations in the last exon lead to truncated proteins without the carboxyterminal transactivation domain. Additionally, the mutant SOX10 is expressed on top of normal levels of wild-type Sox10 in transgenic animals. This contrasts with the situation in patients where the mutant allele replaces one of the normal alleles.

Therefore, we initiated a complementary study on a mutation that leads to a truncated SOX10. To test whether expression of a truncated Sox10 would result in a PCWH-like disease phenotype in mice, we have generated a mouse model in which the Q377X nonsense mutant is expressed from the *Sox10* locus. This mutant has been associated with neurological phenotypes in the affected human patients including delayed development, cerebral palsy, ataxia and congenital nystagmus (4). The Q377X mutant lacks the complete carboxyterminal transactivation domain and may thus be expected to interfere with the function of wild-type Sox10 and to exert a dominant effect.

Results

Generation of mice expressing the Sox10 Q377X mutant

Using homologous recombination in mouse ES cells, we have previously generated several alleles in which we have replaced the protein-coding exons 3–5 from the *Sox10* gene by a single exon that contains the continuous open reading frame for wild-type or mutant Sox10 proteins (17, 18). This exon is faithfully spliced to the preceding two exons. The resulting mRNA is translated in the expected spatiotemporal pattern and in wild-type levels (17, 18).

To generate the mutant Sox10 Q377X allele ($Sox10^{377X}$), we employed a similar strategy (Fig. 1A–D). We inserted the complete open reading frame for the Sox10 Q377X variant into exon 3 in such a way that the translation start for the mutant was at the wild-type position, and deleted all wild-type sequences behind the translation start (Fig. 1A). Additionally, we inserted a floxed neomycin cassette with three polyadenylation sites into intron 2. This stopflox cassette causes premature termination of transcription and thus prevents protein production from the mutant *Sox10* locus.

Using homologous recombination, we generated ES cell clones that had one mutant *Sox10* allele ($Sox10^{Sfl}$) with stopflox cassette (Fig. 1B). $Sox10^{+/Sfl}$ mice were produced from one correctly recombined ES cell clone (Fig. 1C). Immunohistochemistry on $Sox10^{Sfl/Sfl}$ embryos at E12.5 confirmed that no Sox10 protein is produced from this allele (Fig. 1E). Cre-mediated removal of the stopflox cassette was performed to convert the $Sox10^{Sfl}$ allele into the $Sox10^{377X}$ allele (Fig. 1A and D). In contrast to their $Sox10^{Sfl/Sfl}$ counterparts, $Sox10^{377X/377X}$ embryos exhibited Sox10 immunoreactivity at E12.5 (Fig. 1E). Signal intensity appeared highly similar for immunoreactive cells in wild-type and $Sox10^{377X/377X}$ embryos. However, numbers of immunoreactive cells were only comparable in the CNS but not in dorsal root ganglia and other parts of the PNS because of tissue-specific cell loss (9). Western blots on spinal cord tissue at E18.5 confirmed that a truncated Sox10 variant was produced in $Sox10^{377X/377X}$ embryos instead of the wild-type protein (Fig. 1F).

Ideally, expression levels of the $Sox10^{377X}$ allele should closely resemble that of the wild-type allele. For quantification, we prepared RNA from spinal cord at E18.5 as a tissue where the number of Sox10-expressing cells is unchanged in $Sox10^{377X/377X}$ embryos, and performed quantitative rtPCR. First, we determined the total amount of *Sox10* transcripts using primers that recognized the $Sox10^{377X}$ as well as the wild-type allele. These experiments indicated that *Sox10* transcript levels are 1.35-fold higher in $Sox10^{377X/377X}$ embryos than in wild-type embryos and 1.2-fold higher in $Sox10^{+/377X}$ embryos (Fig. 1G). Primers that selectively recognized the $Sox10^{377X}$ allele only detected *Sox10* transcripts in $Sox10^{+/377X}$ and $Sox10^{377X/377X}$ embryos, whereas primers for the wild-type allele only detected transcripts in wild-type and $Sox10^{+/377X}$ embryos (Fig. 1H and I). At the same time, transcript levels for the *Sox10* paralogs *Sox8* and *Sox9*

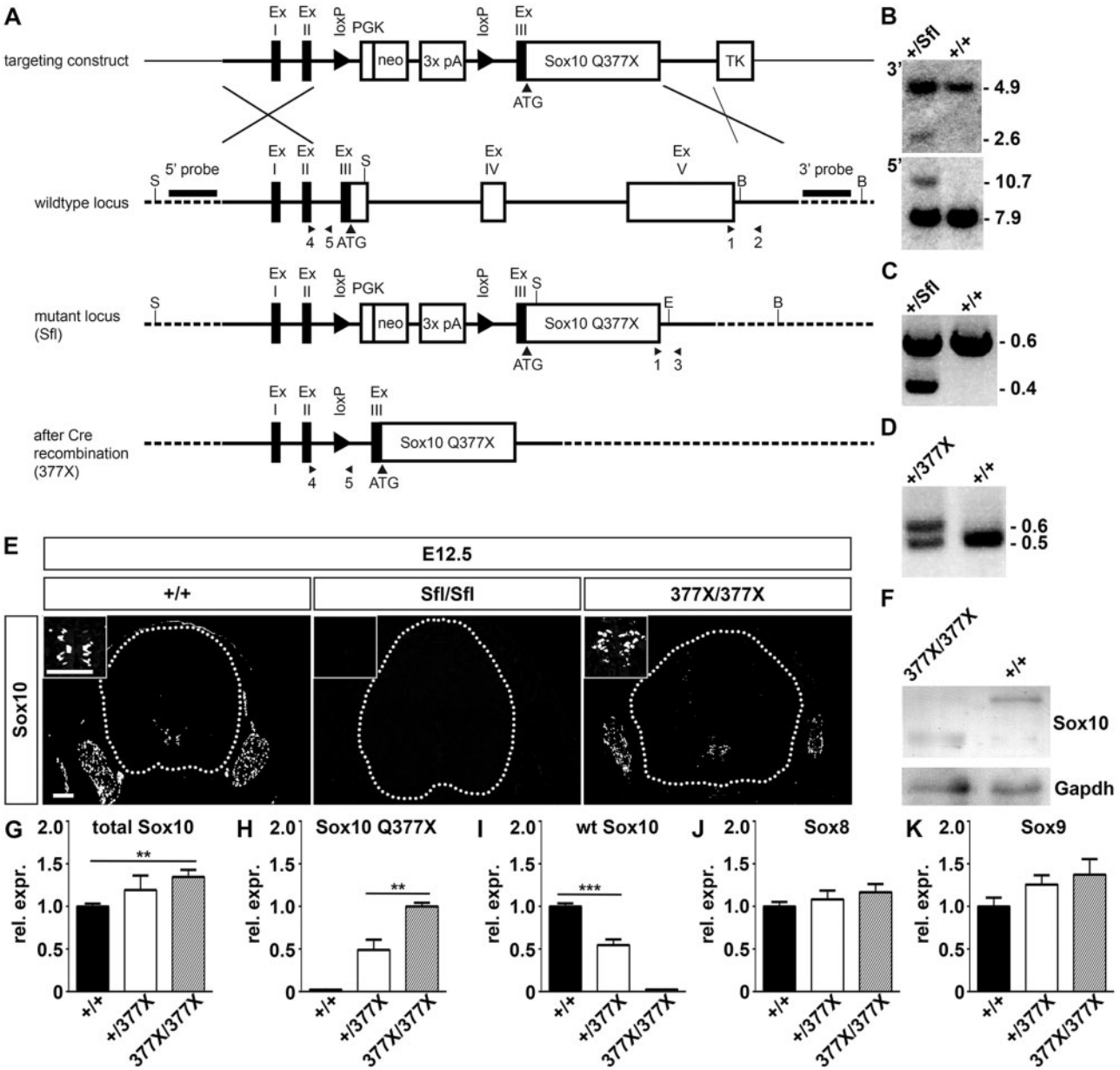

Figure 1. Generation of mice with a *Sox10*^{377X} allele. (**A**) Schematic representation (from top to bottom) of targeting construct, *Sox10* wild-type locus, mutant locus before Cre recombination (corresponding to the stopflox allele *Sox10*^{Sfl}) and *Sox10*^{377X} allele after Cre recombination. The *Sox10* exons (Ex I–V) and the mutant *Sox10* Q377X open reading frame are shown as boxes. The 4.3 and 1.5 kb regions of homology between wild-type locus and targeting vector and introns 3 and 4 are depicted as thick black lines, vector backbone sequences as thin lines, and surrounding genomic regions not contained in the targeting construct as dashed lines. Restriction sites for BamHI (B), EcoRV (E) and SacI (S) are shown, as are the locations of the 5′ and 3′ probes and the start codon of the *Sox10* gene (ATG). The arrowheads below wild-type and mutant *Sox10* loci indicate the locations of primers 1–5 used for PCR genotyping. neo, neomycin resistance cassette; 3x pA, polyadenylation signal; loxP, recognition sites for Cre recombinase; PGK, phosphoglycerate kinase promotor; TK, herpes simplex virus thymidine kinase gene cassette. (**B**) Southern blot analysis of DNA from heterozygous (+/Sfl) and wild-type (+/+) ES cells digested with BamHI and EcoRV for use of the 3′ probe, and with SacI for the 5′ probe. The size of bands corresponding to the wild-type (4.9 kb for the 3′ probe and 7.9 kb for the 5′ probe) and the *Sox10*^{Sfl} allele (2.6 kb for the 3′ probe and 10.7 kb for the 5′ probe) are indicated. (**C, D**) PCR genotyping of wild-type (+/+), *Sox10*$^{+/Sfl}$ (+/Sfl) and *Sox10*$^{+/377X}$ (+/377X) animals at weaning. DNA fragments indicative of the wild-type are 0.6 kb (C) and 0.5 kb (D), whereas the PCR product for the *Sox10*^{Sfl} allele (C) is 0.4 kb and the one for the *Sox10*^{377X} allele (D) 0.6 kb. (**E**) Immunohistochemistry of transverse sections from wild-type (+/+), *Sox10*$^{Sfl/Sfl}$ (Sfl/Sfl) and *Sox10*$^{377X/377X}$ (377X/377X) mice at E12.5 with antibodies directed against Sox10. The circumference of the spinal cord is indicated by a dotted line. The inlay in the upper left corner shows a magnification of the pMN domain of the ventral spinal cord. Size bars, 100 μm. (**F**) Western blot analysis of spinal cord extract from *Sox10*$^{377X/377X}$ and wild-type embryos at E18.5 with antibodies directed against Sox10 and Gapdh as loading control. (**G–K**) Amounts of total *Sox10* (G), *Sox10 Q377X* (H), wild-type *Sox10* (I), *Sox8* (J) and *Sox9* (K) transcripts were compared in spinal cord tissue of wild-type (+/+, black bars), *Sox10*$^{+/377X}$ (+/377X, white bars) and *Sox10*$^{377X/377X}$ (377X/377X, gray bars) embryos at E18.5 by quantitative rtPCR. After normalization to *Rpl8*, transcript levels in wild-type (G, I–K) or *Sox10*$^{377X/377X}$ (H) embryos were arbitrarily set to 1 and levels in all other gentoypes were expressed relative to it + SEM ($n = 3$). Differences to the respective controls were statistically significant as indicated (Student's *t* test; $^{**}P \leq 0.01$; $^{***}P \leq 0.001$).

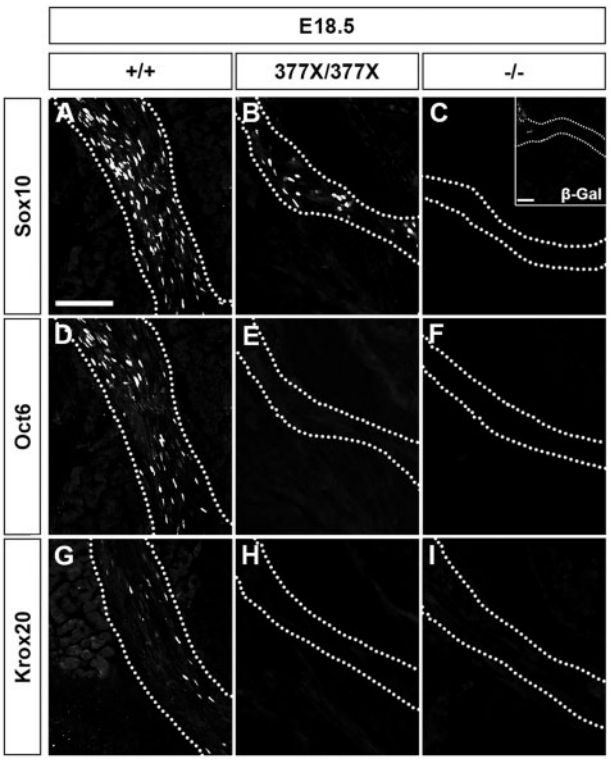

Figure 2. Analysis of Schwann cell development in perinatal peripheral nerves of $Sox10^{377X/377X}$ mice. (**A–I**) Immunohistochemistry was performed on spinal nerves of wild-type (+/+; A, D, G), $Sox10^{377X/377X}$ (377X/377X; B, E, H) and $Sox10^{lacZ/lacZ}$ (−/−; C, F, I) mice at E18.5 with antibodies directed against Sox10 (A–C), Oct6 (D–F), Krox20 (G–I) and β-galactosidase (inlay in C). The nerve area is marked by dotted lines. Size bars, 100 μm.

remained unaltered (Fig. 1J and K). If anything, exchange of the wild-type allele by the $Sox10^{377X}$ allele thus causes a modest increase in *Sox10* expression levels.

Similar to Sox10-deficient ($Sox10^{lacZ/lacZ}$) mice (9), $Sox10^{377X/377X}$ mice were not viable. They died immediately after birth so that analysis of homozygous animals had to be restricted to pre- and perinatal stages.

Effects of Sox10 Q377X on peripheral nerves and PNS myelin

To study the consequences of Sox10 Q377X expression on peripheral nerves, we first analyzed spinal nerves of $Sox10^{377X/377X}$ embryos at E18.5 and compared them with those of age-matched wild-type and $Sox10^{lacZ/lacZ}$ embryos (Fig. 2A–I). At this time, wild-type spinal nerves contain a high number of Sox10-positive Schwann cells (Fig. 2A). Most of them have already entered the promyelinating stage and are Oct6-positive (Fig. 2D). Some have even progressed to the myelinating stage as evident by their Krox20 expression (Fig. 2G). In contrast, spinal nerves of $Sox10^{lacZ/lacZ}$ embryos are devoid of Schwann cells as judged by the absence of β-galactosidase, Oct6 or Krox20 expression (Fig. 2C, F and I). This has been previously described and is due to a failure of Schwann cell specification in the absence of Sox10 (9). Age-matched spinal nerves of $Sox10^{377X/377X}$ embryos are distinct from those of wild-type and $Sox10^{lacZ/lacZ}$ embryos. Schwann cells are detected by expression of the mutant Sox10 but in substantially reduced numbers (Fig. 2B). In fact, only 12 ± 1 Schwann cells were found per 100 μm-long proximal nerve sections in $Sox10^{377X/377X}$ embryos as compared with 54 ± 1 in the wild-type ($n = 3$; $P \leq 0.001$). Oct6 and Krox20 expression is completely missing along nerves of $Sox10^{377X/377X}$ embryos arguing that the remaining Schwann cells are severely delayed in their capacity to differentiate or incapable of differentiation (Fig. 2E and H). Peripheral nerves of $Sox10^{377X/377X}$ mice are also thinner in CNS-proximal regions (2.7 ± 0.5-fold; $n = 3$) and sometimes appear defasciculated in more distal regions (Fig. 2 and data not shown). These PNS defects likely contribute to the perinatal death of $Sox10^{377X/377X}$ mice.

Postnatal analysis had to be restricted to $Sox10^{+/377X}$ mice. On a gross morphological level, $Sox10^{+/377}$ mice phenotypically resembled $Sox10^{+/lacZ}$ mice on a comparable genetic background. When backcrossed on a C3H background, a white belly spot was fully penetrant in $Sox10^{+/377X}$ mice and $Sox10^{+/lacZ}$ mice from second generation onwards, whereas < 5% of $Sox10^{+/377X}$ and $Sox10^{+/lacZ}$ mice succumbed to a megacolon around the time of weaning (19). These phenotypic alterations correspond to Waardenburg and Hirschsprung symptoms observed in human patients heterozygous for the mutation.

To check for additional phenotypic changes that are indicative of peripheral neuropathies, we investigated the PNS in $Sox10^{+/377X}$ mice. Most of the analyses were performed on the sciatic nerve as a well-studied peripheral nerve. First, we compared *Sox10* expression levels in wild-type and $Sox10^{+/377X}$ nerve tissue. Quantitative rtPCR studies showed that total amounts of *Sox10* transcripts in the sciatic nerve were nearly identical in both genotypes at P8, whereas the amount of wild-type transcripts was halved (Fig. 3A and B). This argues that wild-type and mutant allele are expressed at similar levels in the nerve. Amounts of *Sox8* transcripts were also comparable between genotypes and *Sox9* transcripts remained undetectable in $Sox10^{+/377X}$ nerve tissue, indicating that the *Sox10* mutation did not cause a compensatory upregulation of paralogous Sox genes (Fig. 3C and D).

Phenotypic analysis of the sciatic nerve was performed at P3 and P7 as times when myelination is ongoing, P21 as an age where myelination is complete, and P60 as a stage of myelin maintenance. At all stages sciatic nerves of $Sox10^{+/377X}$ mice were compared with those of wild-type mice and $Sox10^{+/lacZ}$ mice with the latter representing the haploinsufficient situation.

At P3, the number of Sox10-expressing Schwann cells in the sciatic nerve of $Sox10^{+/377X}$ mice closely resembled the wild-type (Fig. 3E, F and Q). Numbers in $Sox10^{+/lacZ}$ mice were slightly reduced by 16% (Fig. 3G and Q). However, this reduction did not reach statistical significance and likely reflects a problem of detection as Sox10 levels and intensity of the Sox10 signal are substantially lower in $Sox10^{+/lacZ}$ mice. The number of myelinating Schwann cells are comparable among all three genotypes as no differences were detected for Krox20, Mbp or Mpz as markers for these cells (Fig. 3H–P and R–T).

We failed to detect substantial numbers of Sox2-positive cells in the sciatic nerve of any genotype (Fig. 3U). In the wild-type, expression of Sox2 as a marker for the immature Schwann cell stage is dramatically reduced before birth, and its postnatal presence is usually associated with pathological alterations or regenerative events. The absence of Sox2 in sciatic nerves of $Sox10^{+/377X}$ and $Sox10^{+/lacZ}$ mice at P3 argues against major disturbances of Schwann cell development at this time. This conclusion is also supported by the number of Iba1-positive macrophages in the nerves of $Sox10^{+/377X}$ and $Sox10^{+/lacZ}$ mice, which is low and comparable to the wild-type (Fig. 3V).

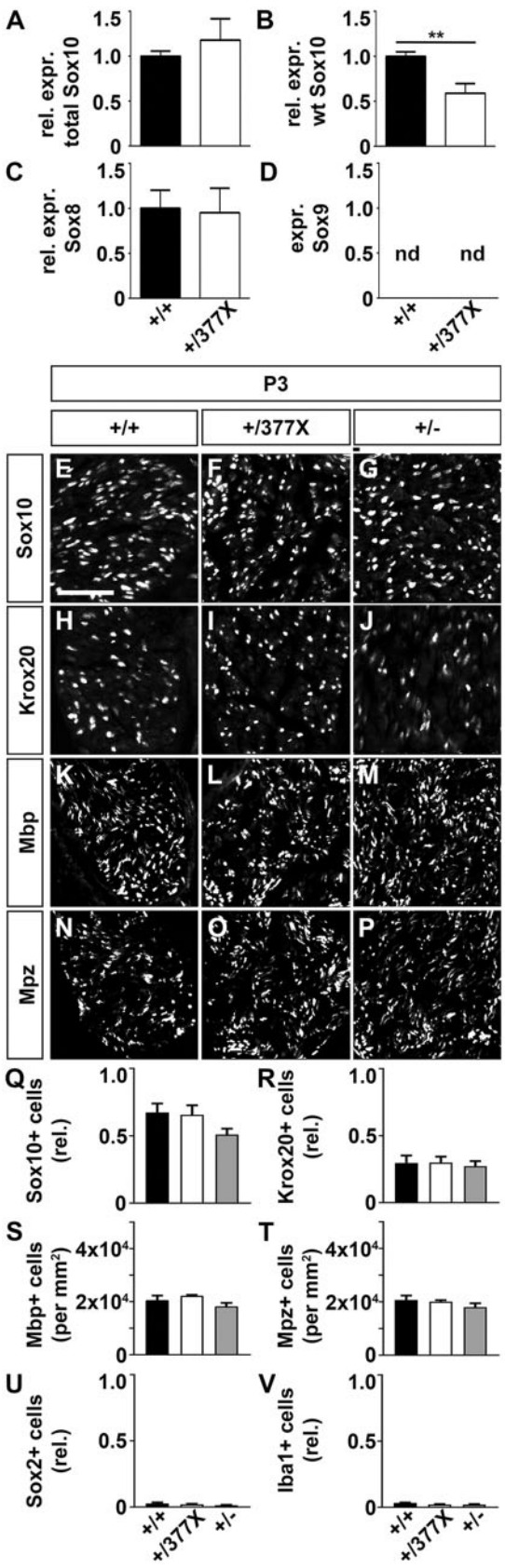

Figure 3. Analysis of Schwann cell development in the early postnatal sciatic nerve of $Sox10^{+/377X}$ mice. (**A–D**) Quantitative rtPCR was performed to determine the amounts of total *Sox10* (A), wild-type *Sox10* (B), *Sox8* (C) and *Sox9* (D) transcripts in the sciatic nerve of wild-type (+/+) and $Sox10^{+/377X}$ (+/377X) mice at P8. After normalization to *Rpl8*, total and wild-type *Sox10* as well as *Sox8* transcript levels in wild-type mice were arbitrarily set to 1 and levels in $Sox10^{+/377X}$ mice were expressed relative to it + SEM (A–C, $n = 3$). *Sox9* transcripts were not detected (nd) (D, $n = 3$). (**E–P**) Immunohistochemistry was performed on sciatic nerves of wild-type (+/+; E, H, K, N), $Sox10^{+/377}$ (+/377X; F, I, L, O) and $Sox10^{+/lacZ}$ (+/−; G, J, M, P) mice at P3 with antibodies directed against Sox10 (E–G), Krox20 (H–J), Mbp (K–M) and Mpz (N–P). Size bar, 50 μm. (**Q–V**) From these and similar stainings, quantifications of cells positive for Sox10 (Q), Krox20 (R), Mbp (S), Mpz (T), Sox2 (U) and Iba1 (V) were performed on sciatic nerves from three pups for each genotype ($n = 3$) counting three separate sections. Presentations are as fraction of all 4′, 6-diamidin-2-phenylindole (DAPI)-positive cells in the nerve (Q, R, U, V) or as absolute cell numbers per mm^2 (S, T). Statistically significant differences between mutant genotypes and wild-type were determined by two-tailed Student's *t*-test (**$P \leq 0.01$).

Similar studies were also carried out at P7, P21 and P60 (Fig. 4A–E). None of the analyzed Schwann cell markers pointed to alterations in number (Sox10, Fig. 4A) or differentiation status (Krox20 versus Sox2, Fig. 4B and C). Expression of myelin genes such as Mbp and Mpz was comparable among the three analyzed genotypes at all time points (Fig. 4D and data not shown). Inflammatory changes were not detected and numbers of Iba1-positive macrophages were not higher in sciatic nerves of $Sox10^{+/377X}$ and $Sox10^{+/lacZ}$ mice than wild-type mice (Fig. 4E and data not shown).

Ultrastructural analysis of sciatic nerves at P60 failed to reveal substantial differences among genotypes (Fig. 5A). The distribution of large and small caliber axons was comparable for sciatic nerves of $Sox10^{+/377X}$, $Sox10^{+/lacZ}$ and wild-type mice (Fig. 5B). G ratios pointed to a similar thickness of the myelin sheaths (Fig. 5C and D). Remak bundles looked normal in the mutation-carrying heterozygous $Sox10^{+/377X}$ and $Sox10^{+/lacZ}$ mice (Fig. 5A). We conclude from our histochemical, histological and ultrastructural analyses that development and maintenance of Schwann cells and PNS myelin are normal in $Sox10^{+/377X}$ and $Sox10^{+/lacZ}$ mice.

Effects of Sox10 Q377X on spinal cord, brain and CNS myelin

To extend our study to the CNS, we studied oligodendroglial cells in the spinal cord and looked for signs of dys- or demyelination in mice that express the Sox10 Q377X mutant protein. We started out with an analysis of the spinal cord of $Sox10^{377X/377X}$ embryos at E18.5 in comparison to age-matched wild-type and $Sox10^{lacZ/lacZ}$ embryos (Figs 6A–U and 7A–G). At this age, Olig2- and Sox10-positive oligodendroglial cells are evenly distributed throughout the parenchyma of the wild-type spinal cord (Fig. 6A and D). These cells also express Sox9 and Sox8 (Fig. 6G and J). Most of the cells furthermore correspond to Pdgfra-expressing oligodendrocyte precursor cells (OPCs) (Fig. 6M) rather than maturing Mbp and Plp1-expressing oligodendrocytes (Fig. 6P and S).

When $Sox10^{lacZ/lacZ}$ embryos were analyzed, no differences were observed in number and distribution of Olig2-positive cells (Figs 6C and 7A). The loss of Sox10 (Figs 6F and 7B) was not appreciably compensated by increases of Sox9 or Sox8 (Figs 6I and L and 7C and D). There was no difference in the number of *Pdgfra*-expressing OPCs (Figs 6O and 7E). What was altered in the spinal cord of $Sox10^{lacZ/lacZ}$ embryos was the number of cells that have already started to express myelin genes such as *Mbp* and *Plp1* (Figs 6R and U and 7F and G). These were almost absent confirming previous results that Sox10 is required for myelin gene expression and the initiation of terminal differentiation in oligodendrocytes (12, 20).

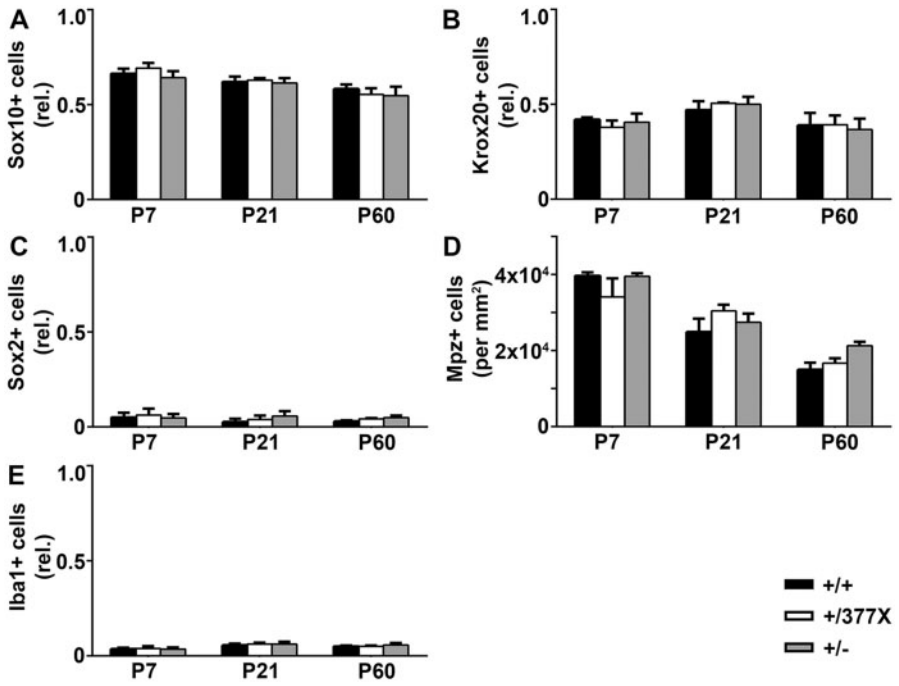

Figure 4. Analysis of Schwann cell development in the postnatal sciatic nerve of *Sox10*$^{+/377X}$ mice. **(A–E)** From immunohistochemical stainings similar to the ones presented in Figure 3, quantifications of cells positive for Sox10 (A), Krox20 (B), Sox2 (C), Mpz (D) and Iba1 (E) were performed on sciatic nerves from wild-type (+/+; black bars), *Sox10*$^{+/377}$ (+/377X; white bars) and *Sox10*$^{+/lacZ}$ (+/−; gray bars) mice at P7, P21 and P60. Three mice were used for each genotype and time point, and three separate sections were counted for each nerve. Mice were treated as biological replicates ($n = 3$). Presentations are as fraction of all DAPI-positive cells in the nerve (A–C, E) or as absolute cell numbers per mm^2 (D). No statistically significant differences between heterozygous mutant genotypes and the wild-type were detected by two-tailed Student's *t*-test.

Olig2- and Sox10-positive oligodendroglial cells in the spinal cord of *Sox10*$^{377X/377X}$ embryos were also present in wild-type numbers (Figs 6B and E and 7A and B). Sox9 and Sox8 expression equaled wild-type levels (Figs 6H and K and 7C and D) and most oligodendroglial cells were in the OPC stage as indicated by *Pdgfra* expression (Figs 6N and 7E). Compared with the wild-type, the number of *Mbp* and *Plp1*-expressing oligodendrocytes was strongly reduced in *Sox10*$^{377X/377X}$ mice (Fig. 6Q and T). Despite the strong decrease, numbers were, however, substantially higher than in *Sox10*$^{lacZ/lacZ}$ embryos (Fig. 7F and G). This was surprising as it points to residual function in the Sox10 Q377X mutant protein.

To assess the impact of the Sox10 Q377X mutant on postnatal oligodendroglial development and homeostasis, we again had to turn to heterozygous mice. We first determined Sox10 expression levels in the spinal cord of *Sox10*$^{+/377X}$ relative to wild-type mice. Quantitative rtPCR revealed that amounts of all *Sox10* transcripts were comparable between genotypes, whereas amounts of wild-type *Sox10* transcripts were only half as high in *Sox10*$^{+/377X}$ mice than in wild-type mice at P8 (Fig. 8A and B). There was no compensatory upregulation of Sox8 or Sox9 in the spinal cord of *Sox10*$^{+/377X}$ mice (Fig. 8C and D).

Time points chosen for the following analysis of oligodendrocyte development and homeostasis were identical to those for Schwann cells in the PNS. Again, *Sox10*$^{+/lacZ}$ mice were included. At P3, the number of cells marked by Olig2 and Sox10 and thus belonging to the oligodendroglial lineage were comparable among all three genotypes (Fig. 8E–J, T and U). In contrast, differences were detected for *Plp1* and Myrf as markers of cells that have started differentiation and initiated myelin gene expression (Fig. 8K–P, V and W). Their number was decreased in the spinal cord of *Sox10*$^{+/377X}$ and *Sox10*$^{+/lacZ}$ mice relative to the wild-type (Fig. 8V and W). However, there was no differences between *Sox10*$^{+/377X}$ and *Sox10*$^{+/lacZ}$ mice. The number of Pdgfra-positive OPCs was comparable among all three genotypes (Fig. 8Q–S and X). There were also no changes in the number of Ki67-positive proliferating or cleaved caspase 3-positive cells undergoing apoptosis (Fig. 8Y and Z).

As postnatal spinal cord development proceeds, more and more oligodendroglial cells differentiate and produce myelin, whereas the fraction of OPCs decreases until a steady state is achieved at P60. The total number of oligodendroglial cells in *Sox10*$^{+/377X}$ and *Sox10*$^{+/lacZ}$ mice remained comparable to the wild-type throughout postnatal spinal cord development (Fig. 9A and B). OPC numbers also exhibited no major alterations among genotypes (Fig. 9E). The minor differentiation defect that we observed in *Sox10*$^{+/377X}$ and *Sox10*$^{+/lacZ}$ mice at P3 (Fig. 8V and W) was no longer visible at any of the later stages (Fig. 9C and D) arguing that oligodendroglial differentiation is only transiently delayed in the heterozygous mice. There were also no alterations in Gfap or Iba1 immunoreactivity as indicators of astrogliosis or microgliosis in the spinal cord of heterozygous mice at any of the analyzed time points (data not shown).

In line with immunohistochemical findings, ultrastructural analysis of myelination in the spinal cord revealed no major abnormalities in the number and size distribution of axons, the structure and compaction of myelin or the g ratio (Fig. 10A–D). We thus conclude that myelination is largely normal in the spinal cord of *Sox10*$^{+/377X}$ mice except for a mild transient delay in the first postnatal days. This delay is comparable to the one observed in *Sox10*$^{+/lacZ}$ mice.

We completed our study by characterizing oligodendroglial cells in the brain. We focused on the forebrain region and analyzed their number and their state of differentiation in cortex

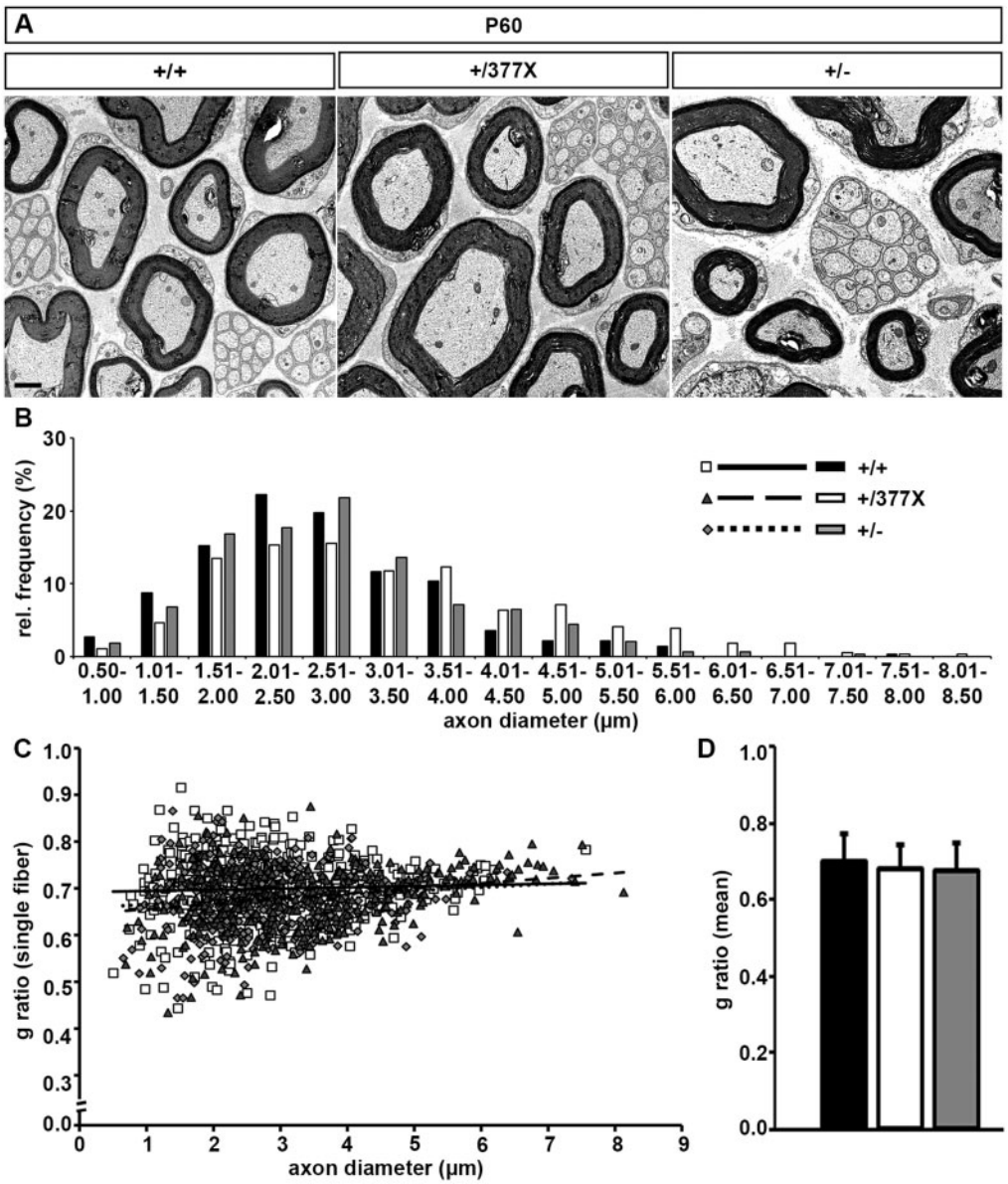

Figure 5. Electronmicroscopic analysis of the sciatic nerve in *Sox10*$^{+/377X}$ mice. (**A**) Sciatic nerve ultrastructure was similar in wild-type (+/+), *Sox10*$^{+/377}$ (+/377X) and *Sox10*$^{+/lacZ}$ (+/−) mice at P60, each showing densely packed large caliber myelinated axons and interspersed Remak bundles. Size bar, 1 µm. (**B–D**) Morphometric analysis of myelination in sciatic nerves of wild-type (+/+), *Sox10*$^{+/377}$ (+/377X) and *Sox10*$^{+/lacZ}$ (+/−) mice at P60. Axon diameter and g ratio were determined in sciatic nerve sections to analyze the relative distribution of axon diameters (B), the correlation of axon diameter and g ratio for single fibers (scatter blot in C) and the mean g ratio per genotype (bar graph in D).

and corpus callosum at P7, P21 and P60. We did not detect any significant differences in the number of Olig2-positive oligodendroglial cells among the three genotypes at any of the analyzed time points (Fig. 11A and B). For Sox10, a slight reduction was observed only at P7 in the corpus callosum of *Sox10*$^{+/lacZ}$ mice (Fig. 11C and D). Again, this is likely due to a detection problem resulting from reduced Sox10 amounts per cell in this genotype. Differentiating and myelin producing oligodendrocytes were present in slightly lower numbers at P7 in both *Sox10*$^{+/377X}$ and *Sox10*$^{+/lacZ}$ mice as evident from Myrf and *Plp1* expression (Fig. 11E–H). The effect was on the verge of being statistically significant. However, reductions were transient and no longer observed at P21 or P60. The number of Pdgfra-positive OPCs were similar in the three genotypes at all analyzed time points (Fig. 11I and J). We conclude from these studies that the consequences of heterozygous Sox10 mutation or loss are comparable for the oligodendroglial population in forebrain and spinal cord. No evidence was obtained for a dominant function of the Sox10 Q377X mutation in brain or spinal cord of *Sox10*$^{+/377X}$ mice.

Discussion

In this study, we have generated mice that carry a *Sox10*^{377X} allele. In humans, this allele caused PCWH-like neurological symptoms in the two heterozygously affected siblings in whom it was identified (4). Considering the exclusive expression of

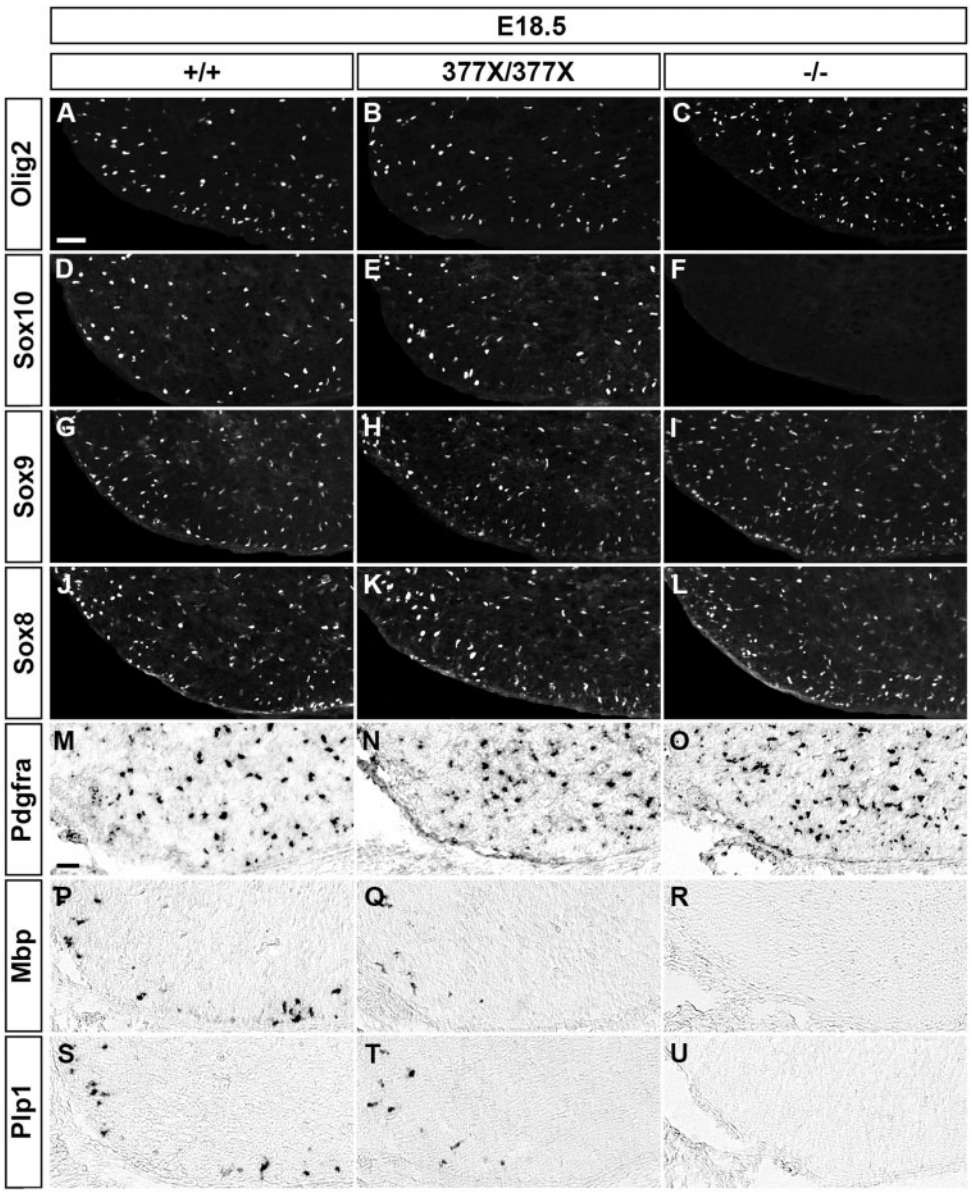

Figure 6. Analysis of oligodendrocyte development in the spinal cord of *Sox10*$^{377X/377X}$ mice. **(A–L)** Immunohistochemistry was performed on spinal cord tissue of wild-type (+/+; A, D, G, J), *Sox10*$^{377X/377X}$ (377X/377X; B, E, H, K) and *Sox10*$^{lacZ/lacZ}$ (−/−; C, F, I, L) mice at E18.5 with antibodies directed against Olig2 (A–C), Sox10 (D–F), Sox9 (G–I) and Sox8 (J–L). **(M–U)** *In situ* hybridization was performed on spinal cord tissue of wild-type (M, P, S), *Sox10*$^{377X/377X}$ (N, Q, T) and *Sox10*$^{lacZ/lacZ}$ (O, R, U) mice at E18.5 with antisense riboprobes specific for *Pdgfra* (M–O), *Mbp* (P–R) and *Plp1* (S–U). The ventral right segment of the spinal cord is shown, for immunohistochemical stainings placed on a black background. Size bars, 100 μm.

Sox10 in myelinating glia of PNS and CNS and the phenotype in Sox10-deficient mouse mutants (9, 12, 21), symptoms should be caused by cell-intrinsic abnormalities in myelinating glia. Using *Sox10*$^{+/377X}$ mice, we addressed the question whether the neurological phenotype of patients is reproduced in mice and can be detected as abnormalities in Schwann cells, oligodendrocytes or their myelin.

Sox10$^{+/lacZ}$ mice do not exhibit abnormalities in peripheral or central glia. They present with a combination of pigmentation and enteric nervous system defects that are comparable to combined Waardenburg–Hirschsprung disease (WS4) in human patients and typical for the haploinsufficient situation (3, 4, 9). Detection of glial defects in *Sox10*$^{+/377X}$ mice would have supported the assumption that the mutant Sox10 protein exerts dominant effects, and by extrapolation that the combination of neurological symptoms with Waardenburg–Hirschsprung disease in PCWH is a result of the presence of such dominant SOX10 proteins in patients.

Somewhat to our surprise, we failed to detect any evidence for such dominant function in PNS or CNS. Despite clear evidence for the presence of substantial amounts of the mutant Sox10 protein and wild-type expression levels of the *Sox10*^{377X} allele, no major abnormalities were observed in *Sox10*$^{+/Q377X}$ mice regarding development and maintenance of Schwann cells and oligodendrocytes or regarding generation and homeostasis of myelin. We only detected a slight and transient delay in oligodendroglial differentiation during the first postnatal days. However, this was similarly observed in *Sox10*$^{+/lacZ}$ mice as

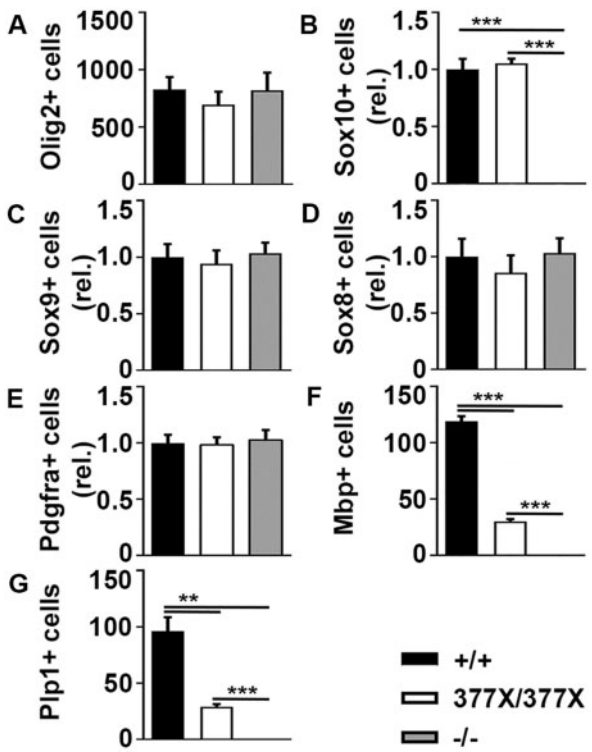

Figure 7. Quantification of oligodendroglial markers in the spinal cord of $Sox10^{377X/377X}$ mice. (**A–G**) From immunohistochemical stainings and *in situ* hybridizations similar to the ones presented in Figure 6, quantifications of cells positive for Olig2 (A), Sox10 (B), Sox9 (C), Sox8 (D), Pdgfra (E), Mbp (F) and Plp1 (G) were performed on spinal cord tissue from wild-type (+/+; black bars), $Sox10^{377X/377X}$ (377X/377X; white bars) and $Sox10^{lacZ/lacZ}$ (−/−; gray bars) mice at E18.5. Three mice were used for each genotype, and three separate sections were counted for each nerve. Mice were treated as biological replicates ($n = 3$). Presentations are as absolute numbers of marker-positive cells per spinal cord section (A, F, G) or as relative numbers (B–E) with marker-positive cells per section in the wild-type arbitrarily set to 1. Statistically significant differences between heterozygous mutant genotypes and the wild-type were determined by two-tailed Student's *t*-test (*$P \leq 0.05$; **$P \leq 0.01$; ***$P \leq 0.001$).

previously reported (22), and thus cannot be taken as indication for a dominant function of the Sox10 Q377X mutant protein. The residual number of Schwann cells along the peripheral nerves of $Sox10^{Q377X/Q377X}$ embryos and the few differentiating oligodendrocytes detected in the spinal cord rather argue for a residual functionality of the mutant Sox10 protein.

The results are surprising because we would have expected that the presence of a mutant Sox10 that has retained its DNA-binding ability but lost its major transactivation domain (23), should at least interfere with the function of the wild-type Sox10 protein. The simplest explanation for the lack of such a dominant-negative function may be a dramatically lower expression of the mutant Sox10 relative to the wild-type version. However, our immunohistochemical and rtPCR data argue against that. We favor a different explanation. For one, the Sox10 Q377X mutant has retained a second internal and weaker transactivation domain, the so called K2 domain (17). This K2 domain is required for Schwann cell differentiation and also has a minor impact on oligodendroglial differentiation and myelin gene expression *in vivo* (17). It may thus be responsible for partial retention of transactivation capacity in the Sox10 Q377X mutant. Such residual activity may also explain why myelin expression in the perinatal spinal cord of $Sox10^{Q377X/Q377X}$ embryos is not as severely reduced as in $Sox10^{lacZ/lacZ}$ embryos. It also has to be taken into consideration that Sox10 performs many of its functions as homodimer and possibly as heterodimer with the related Sox9 and Sox8 (24, 25). Previous work had also shown that a functional dimerization domain is essential for Sox10 function in Schwann cell differentiation and peripheral myelination *in vivo* (17). The Sox10 Q377X mutant is still capable of dimerization. Heterodimers between wild-type and mutant Sox10 still contain a transactivation domain and such a dimer may still be fully or partially active.

As surprising as they may be, our results are consistent with previously published data on this and other Sox10 truncation mutants. For one, the Sox10 Q377X mutant has previously been tested for its impact on neural crest development in chicken following in ovo electroporation (26). Despite the very high levels usually reached during electroporation for the ectopically expressed protein, these studies failed to reveal any evidence of a dominant action for the Sox10 Q377X variant. Instead, it rather behaved like an inactive protein.

Additionally, there have also been reports that the Sox10 frameshift mutation in Dom mice, that has been instrumental in the original identification of Sox10 as a WS4-associated gene (10, 11), leads to the production of a mutant Sox10 protein *in vivo*. In this mutant, the first 193 amino acids are followed by 99 additional amino acids that are not normally found in Sox10 (27). Although it may have reduced DNA-binding activity, it is generally capable of DNA-binding (26, 27). Still, $Sox10^{+/dom}$ mice do not differ phenotypically from $Sox10^{+/lacZ}$ mice provided they are kept on an identical genetic background. Thus, there is precedence that a *Sox10* mutation that leads to a truncated protein *in vivo* does not function in a dominant fashion in mice.

Our study thus comes to conclusions that are different from Ito *et al.* (15) who analyzed the phenotypic consequences of expression of a *SOX10 c.1400del12* transgene that produces a mutant Sox10 with extended open reading frame. It has to be kept in mind that this mutation is very different from the truncated Sox10 Q377X analyzed in our study, and may thus behave differently. Additionally, it also needs to be emphasized that the experimental setup is different in the two studies. Whereas the *Sox10 Q377X* allele in our study replaces a wild-type allele, the *SOX10 c.1400del12* transgene was expressed on the background of two wild-type alleles.

Many studies provide evidence that Sox10 function is strongly dose-dependent. As a result even overexpression of wild-type Sox10 may cause phenotypic abnormalities, and the study by Ito *et al.* (15) cannot distinguish between consequences of overexpression of the mutant Sox10 and Sox10 overexpression *per se*.

Considering that we do not find abnormalities in glial cells and myelin of PNS and CNS in heterozygous mice, it seems unlikely that there is a strict correlation between nonsense-/frameshift mutations in the last exon, escape from NMD of the mutant transcript, expression of a dominant SOX10 and a PCWH-like phenotype. Our results would rather argue that the phenotypic manifestation of a particular SOX10 mutation is multifactorial and that the genetic background and modifiers are not only involved in the decision between Waardenburg, Hirschsprung and Waardenburg–Hirschsprung disease (7) but are also an essential factor in the manifestation of PCWH.

In this respect, it needs to be emphasized that our studies were conducted in mice on a mixed, largely C3H background. As modifiers are known to have a substantial impact on the phenotypic manifestation of Sox10 mutations in mice (4, 28, 29), we cannot exclude that neurological symptoms would become

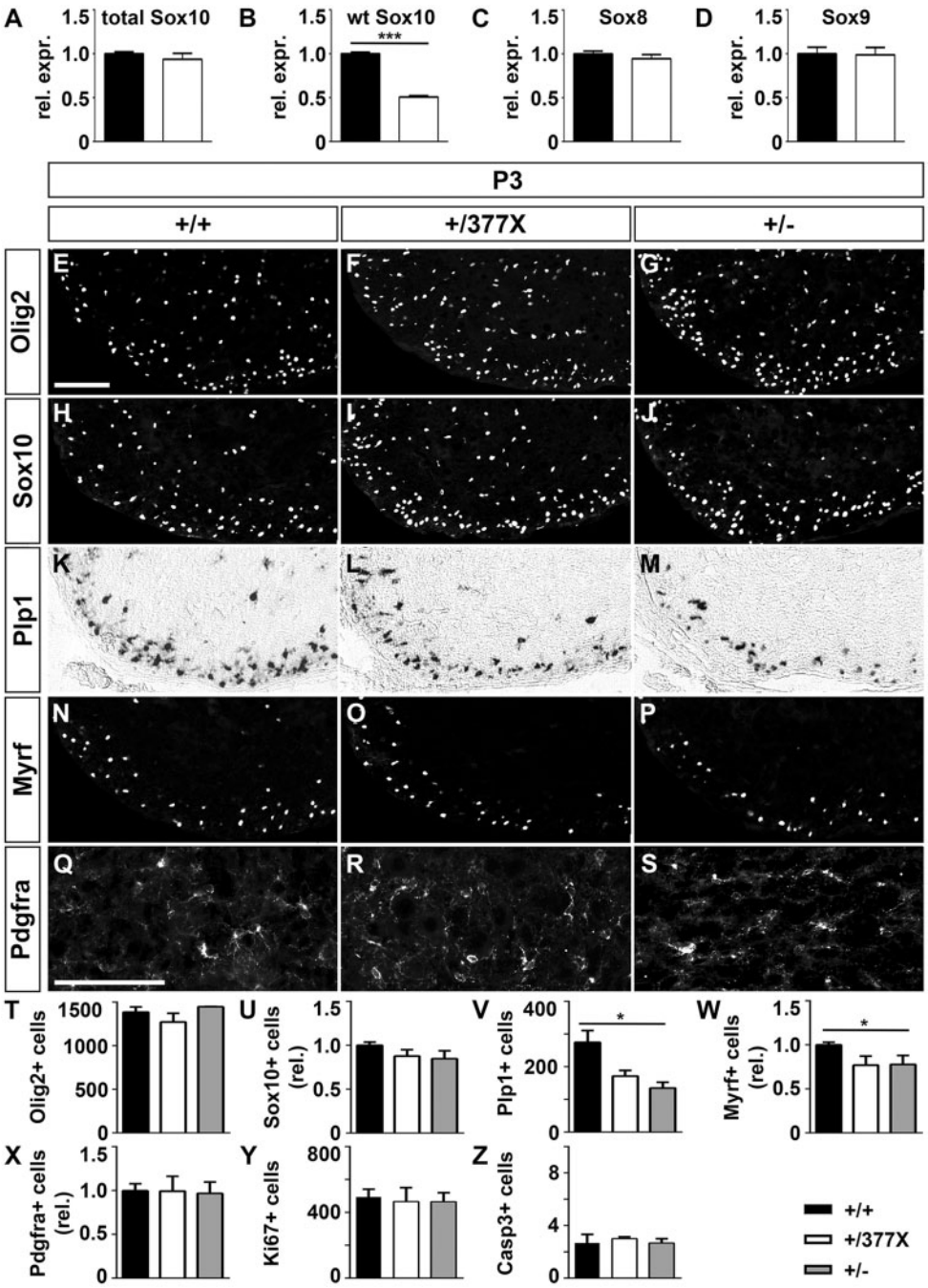

Figure 8. Analysis of oligodendrocyte development in the early postnatal spinal cord of *Sox10*$^{+/377X}$ mice. (**A–D**) Quantitative rtPCR was performed to determine the amounts of total *Sox10* (A), wild-type *Sox10* (B), *Sox8* (C) and *Sox9* (D) transcripts in the spinal cord of wild-type (black bars) and *Sox10*$^{+/377X}$ (white bars) mice at P8. After normalization to *Rpl8*, transcript levels in wild-type mice were arbitrarily set to 1 and levels in *Sox10*$^{+/377X}$ mice were expressed relative to it + SEM ($n = 4$). (**E–S**) Immunohistochemical stainings (E–J, N–S) and *in situ* hybridizations (K–M) were performed on spinal cord tissue of wild-type (+/+; E, H, K, N, Q), *Sox10*$^{+/377}$ (+/377X; F, I, L, O, R) and *Sox10*$^{+/lacZ}$ (+/−; G, J, M, P, S) mice at P3 using antibodies directed against Olig2 (E–G), Sox10 (H–J), Myrf (N–P) and Pdgfra (Q–S) as well as *Plp1*-specific riboprobe (K–M). The ventral right segment of the spinal cord (E–P) or a region from the ventral gray matter (Q–S) are shown, for immunohistochemical stainings placed on a black background. Size bars, 100 μm. (**T–Z**) From these and similar stainings, quantifications of cells positive for Olig2 (T), Sox10 (U), *Plp1* (V), Myrf (W), Pdgfra (X), Ki67 (Y) and cleaved caspase 3 (Z) were performed on spinal cord sections from wild-type (+/+; black bars), *Sox10*$^{+/377}$ (+/377X; white bars) and *Sox10*$^{+/lacZ}$ (+/−; gray bars) mice at P3. Three mice were used for each genotype, and three separate spinal cord sections were counted. Mice were treated as biological replicates ($n = 3$). Presentations are as absolute numbers of marker-positive cells per spinal cord section (T, V, Y, Z) or as relative numbers (U, W, X) with marker-positive cells per section in the wild-type arbitrarily set to 1. Statistically significant differences between heterozygous mutant genotypes and the wild-type were determined by two-tailed Student's *t*-test (*$P \leq 0.05$; ***$P \leq 0.001$).

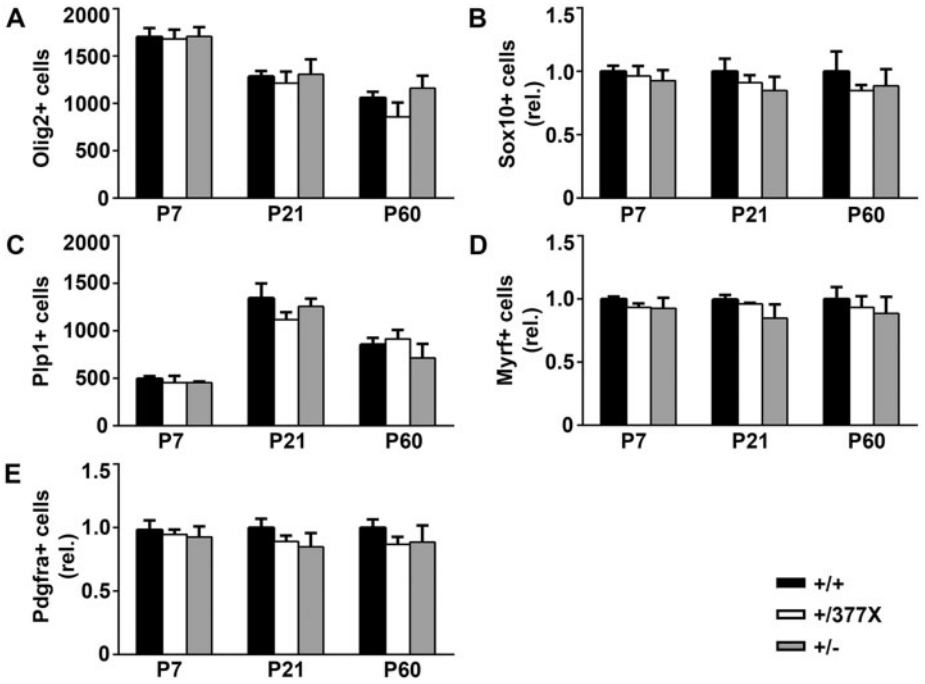

Figure 9. Analysis of oligodendrocytes in the postnatal spinal cord of *Sox10*$^{+/377X}$ mice. (**A–E**) From immunohistochemical stainings and *in situ* hybridizations similar to the ones presented in Figure 8, quantifications of cells positive for Olig2 (A), Sox10 (B), *Plp1* (C), Myrf (D) and Pdgfra (E) were performed on spinal cord tissue of wild-type (+/+; black bars), *Sox10*$^{+/377}$ (+/377X; white bars) and *Sox10*$^{+/lacZ}$ (+/−; gray bars) mice at P7, P21 and P60. Three mice were used for each genotype and time point, and three separate sections were counted for each nerve. Mice were treated as biological replicates ($n = 3$). Presentations are as absolute numbers of marker-positive cells per spinal cord section (A, C) or as relative numbers (B, D, E) with marker-positive cells per section in the wild-type arbitrarily set to 1. No statistically significant difference between heterozygous mutant genotypes and the wild-type was detected by two-tailed Student's *t*-test.

apparent on a different genetic background in *Sox10*$^{+/377X}$ mice. Even if this is the case, this would only strengthen our conclusion of a multifactorial cause for the exact disease phenotype resulting from SOX10 mutations.

Materials and Methods

Construction of targeting vectors, gene targeting, generation and genotyping of mouse mutants

Sequences corresponding to a neomycin resistance cassette with flanking loxP sites and the open reading frame for the mutant Sox10 Q377X protein were placed between 5′ and 3′ *Sox10* genomic regions as homology arms (4.3 and 1.5 kb, respectively) in the context of a pPNT vector backbone as described (9, 17). The targeting vector thereby replaced the *Sox10*-coding exons 3–5 by a continuous *Sox10* reading frame with Q377X mutation (Fig. 1A). The simultaneous insertion of a floxed neomycin cassette in intron 2 prevents transcription of all downstream sequences including the *Sox10 Q377X* open reading frame so that the initially generated *Sox10*^{Sfl} allele is a null allele.

The construct was linearized with PacI and electroporated into E14.1 ES cells followed by selection with G418 (400 μg per ml) and gancyclovir (2 μM). Selected ES cell clones were screened by southern blotting with a 0.6 kb 3′ probe, which recognized a 4.9 kb fragment in case of the wild-type allele and a 2.6 kb fragment in case of the mutant allele in genomic DNA digested with BamHI and EcoRV (Fig. 1B). Appropriate integration of the 5′ end of the targeting construct was verified using a 0.6 kb 5′ probe on ES cell DNA digested with SacI. This probe hybridized to a 10.7 kb fragment in the mutant allele as opposed to a 7.9 kb fragment in the wild-type allele (Fig. 1B). Four ES cell clones were obtained that exhibited a correctly recombined allele. Two of these targeted ES cells clones were injected into C57Bl/6J blastocysts to generate chimeras. Germline transmission was achieved in chimeras from one ES cell clone. In the resulting heterozygous mice, the neomycin resistance cassette was removed by *EIIa::Cre*-mediated recombination (30). This converts the *Sox10*^{Sfl} null allele into the *Sox10*^{377X} allele from which the Sox10 Q377X mutant is expressed (Fig. 1A). Sequencing of genomic DNA from the altered *Sox10* locus confirmed that no additional unintended mutations were introduced during cloning. The generation of mutant mice and their analysis were approved by the responsible local committees and government bodies.

Genotyping of the original *Sox10*^{Sfl} and the final *Sox10*^{377X} allele was routinely performed on DNA from tail tips or yolk sacs by PCR. In case of the *Sox10*^{Sfl} allele one forward (5′-GAGGCCT CCTACCCTAACCC-3′) and two reverse primers (5′-CCCACACTA CACCGACCAG-3′ and 5′-AATCGGAACCCTAAAGGGAGC-3′) at the end of exon V (primers 1–3 in Fig. 1A) were used. A 634 bp fragment was indicative of the wild-type allele, a 355 bp fragment of the *Sox10*^{Sfl} allele (Fig. 1C). For the *Sox10*^{377X} allele, two primers (5′-TCAGTCTCGGCTGTCCAGCC-3′ and 5′-CCTGATCCC AACCGTCTCTA-3′, primers 4 and 5 in Fig. 1A) were used with location in intron 2 upstream and downstream the loxP site that remains after Cre-mediated recombination. A 525 bp fragment was indicative of the wild-type allele, a 628 bp fragment of the *Sox10*^{377X} allele (Fig. 1D).

Mice were kept under standard housing conditions with 12:12 h light-dark cycles and continuous access to food and water in accordance with animal welfare laws. They were kept as heterozygotes and backcrossed on a C3H background. Both males and females of generations F2–F5 were used for the study.

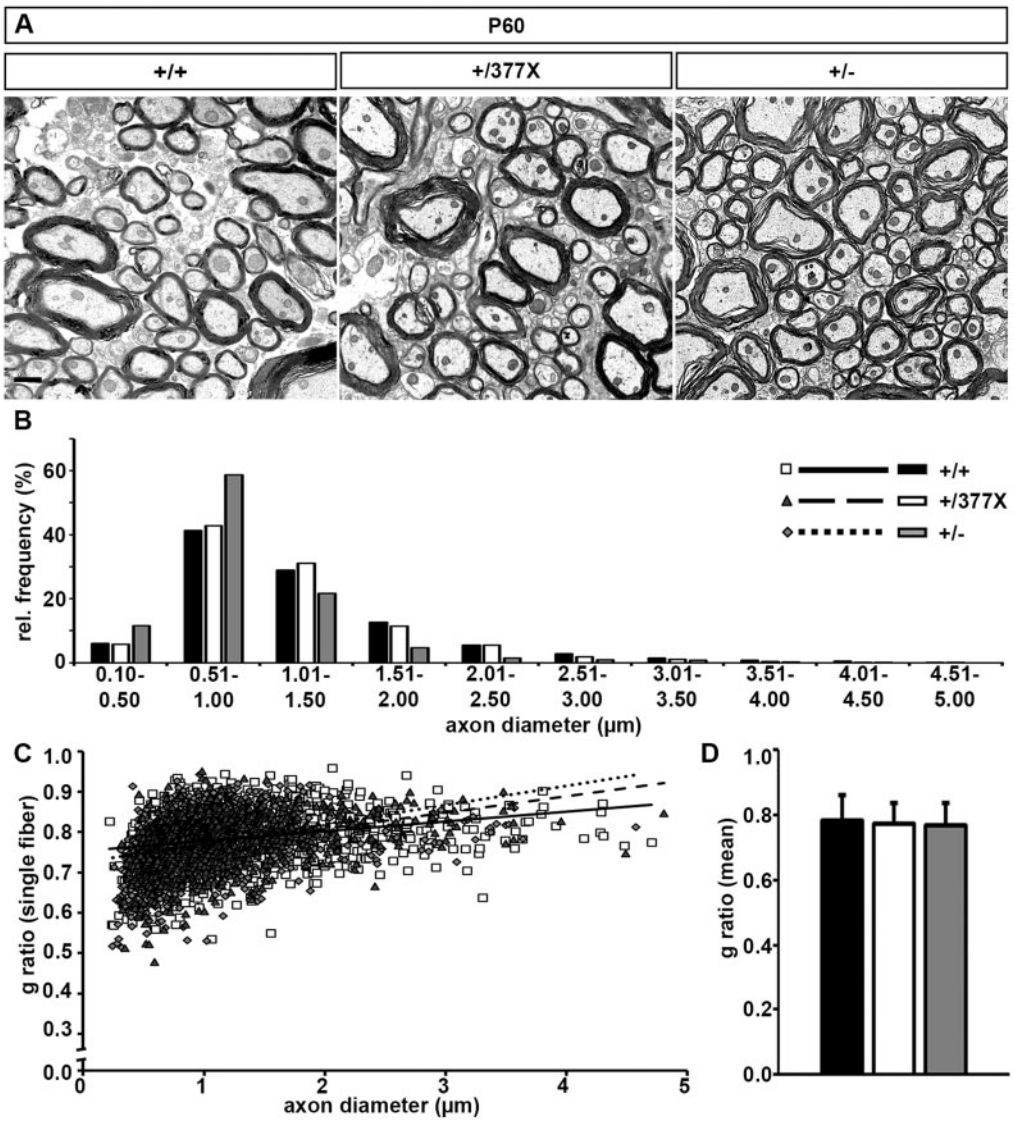

Figure 10. Electronmicroscopic analysis of spinal cord in *Sox10*$^{+/377X}$ mice. (**A**) White matter ultrastructure was similar in spinal cord of wild-type (+/+), *Sox10*$^{+/377}$ (+/377X) and *Sox10*$^{+/lacZ}$ (+/−) mice at P60, each showing densely packed myelinated axons. Size bar, 1 µm. (**B–D**) Morphometric analysis of myelination in spinal cord tissue of wild-type (+/+), *Sox10*$^{+/377}$ (+/377X) and *Sox10*$^{+/lacZ}$ (+/−) mice at P60. Axon diameter and g ratio were determined in spinal cord sections to analyze the relative distribution of axon diameters (B), the correlation of axon diameter and g ratio for single fibers (scatter blot in C) and the mean g ratio per genotype (bar graph in D).

Quantitative rtPCR

RNA was prepared from mouse spinal cord and sciatic nerves at E18.5 and P8, reverse transcribed and used to analyze expression levels by quantitative PCR on a Biorad CFX96 Real Time PCR System. Each spinal cord was separately analyzed, whereas sciatic nerves from two individuals were pooled to obtain sufficient RNA. The following primer pairs were used 5′-ACCT CCACAATGCTGAGCTC-3′ and 5′-CCAGGTGGGCACTCTTGTAG-3′ for all *Sox10* transcripts, 5′-ACAGCAGCAGGAAGGCTTCT-3′ and 5′-TGTCCTCAGTGCGTCCTTAG-3′ for wild-type *Sox10*, 5′-ATCGA CTTCGGCAATGTGGA-3′ and 5′-GGGATCCTCTAGCTTAGGCG-3′ for the *Sox10*^{377X} allele, 5′-ACCCGCATCTCCATAACGCA-3′ and 5′-TGGTGGCCCAGTTCAGTACC-3′ for *Sox8* and 5′-GAACAGAC TCACATCTCTCC-3′ and 5′-TGCTGCTTCGACATCCACAC-3′ for *Sox9*. Transcript levels were normalized to *Rpl8*.

Immunohistochemistry and *in situ* hybridization

Mice were collected as embryos on embryonic day (E) 12.5 and E18.5, as pups on postnatal day (P) 3 and P7, as adolescents at P21 and as young adult at P60. For analysis, tissue was fixed in 4% paraformaldehyde, transferred to 30% sucrose and frozen in Tissue Freezing Medium (Leica). Ten micrometre cryotome sections of spinal cord (at forelimb level), forebrain (level of hippocampal formation) or sciatic nerve (proximal part) were used for immunohistochemistry (18, 31). The following primary antibodies were applied: guinea pig anti-Sox10 antiserum (1:1000 dilution) (19), guinea pig anti-Sox8 antiserum (1:1000 dilution) (32), rabbit anti-Olig2 antiserum (1:1000 dilution, Millipore), rabbit anti-Oct6 antiserum (1:1000 dilution) (33), rabbit anti-Iba 1 antiserum (1:250 dilution, Wako), rabbit anti-Sox9 antibodies (1:2000 dilution) (31), rabbit anti-Pdgfra antiserum (1:300 dilution,

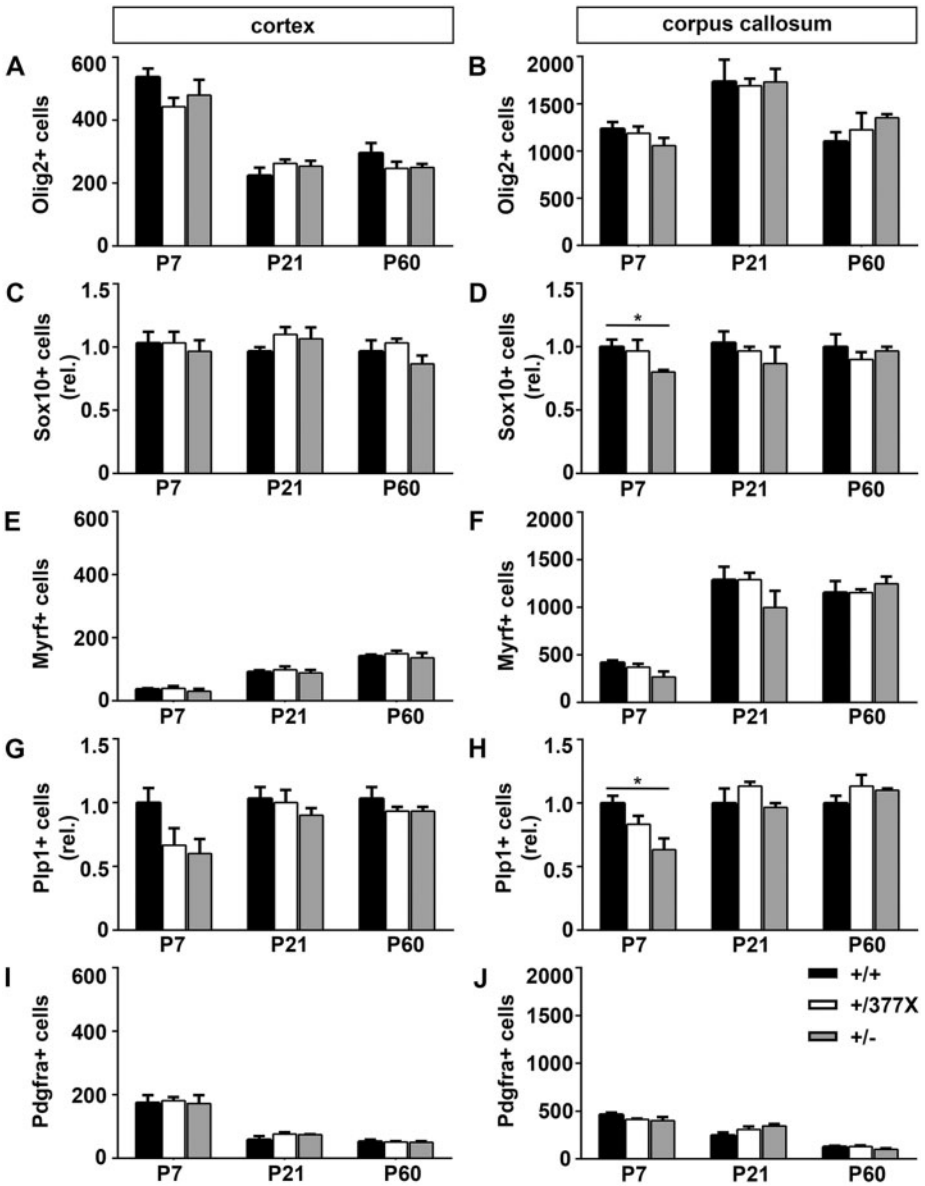

Figure 11. Analysis of oligodendrocytes in the postnatal forebrain of *Sox10*$^{+/377X}$ mice. (**A–J**) From immunohistochemical stainings and *in situ* hybridizations, quantifications of cells positive for Olig2 (A, B), Sox10 (C, D), Myrf (E, F), *Plp1* (G, H) and Pdgfra (I, J) were performed on forebrain tissue of wild-type (+/+; black bars), *Sox10*$^{+/377}$ (+/377X; white bars) and *Sox10*$^{+/lacZ}$ (+/−; gray bars) mice at P7, P21 and P60. Cortex (A, C, E, G, I) and corpus callosum (B, D, F, H, J) were separately analyzed. Three mice were used for each genotype and time point, and three separate sections were counted for each region and brain. Mice were treated as biological replicates. Presentations are as absolute numbers of marker-positive cells per mm^2 (A, B, E, F, I, J) or as relative numbers (C, D, G, H) with marker-positive cells per section in the wild-type arbitrarily set to 1. Statistically significant differences between heterozygous mutant genotypes and the wild-type were determined by two-tailed Student's *t*-test (*$P \leq 0.05$).

Santa-Cruz Biotechnology), rabbit anti-Krox20 antiserum (1:200 dilution, Covance), rabbit anti-Myrf antiserum (1:1000 dilution) (20), rabbit anti-cleaved caspase 3 antiserum (1:200 dilution, Cell Signaling Technology), rabbit anti-Ki67 antiserum (1:500 dilution, Thermo Fisher Scientific), goat anti-Sox2 antiserum (1:500 dilution, Santa Cruz Biotechnology), goat anti-β-galactosidase antibodies (1:500 dilution, Bio Trend), mouse anti-Gfap monoclonal antibodies (1:500 dilution, LabVision/NeoMarkers), rat anti-Mbp antibodies (1:500 dilution, Serotec) and chicken anti-Mpz antibodies (1:2000 dilution; Aves Labs). Secondary antibodies were coupled to Cy3, Cy5 (Dianova) or Alexa488 (Millipore) fluorescent dyes. Nuclei were counterstained with 4′, 6-diamidin-2-phenylindole. Samples were documented with a Leica DMI 6000B inverted microscope (Leica) equipped with a DFC 360FX camera (Leica).

For *in situ* hybridization, 10 μm cryotome sections from spinal cord were incubated with DIG-labeled antisense riboprobes specific for *Pdgfra*, *Mbp* and *Plp1* as described (12, 34). Samples were analyzed and documented with a Leica MZFLIII stereomicroscope equipped with an Axiocam (Zeiss).

Electron microscopy

Spinal cord and sciatic nerve from P60 mice was processed for transmission electron microscopy as described (18). Briefly,

dissected tissues underwent fixation in cacodylate-buffered fixative containing 2.5% paraformaldehyde and 2.5% glutaraldehyde, followed by postfixation in cacodylate-buffered 1% osmium ferrocyanide, dehydration and embedding in Epon resin. Ultrathin sections (50 nm thickness) were stained with uranyl acetate and lead citrate and examined with a Zeiss Libra electron microscope (Carl Zeiss, Inc.). From electron microscopic picture, axon diameters and g ratios were determined as described (18).

Protein extracts and western blotting

Whole-cell protein extracts were prepared from spinal cord tissue of embryos at E18.5 as described (21). Protein extracts from wild-type and homozygous mutant littermates were size-fractionated on polyacrylamide-SDS gels, blotted onto nitrocellulose membranes and analyzed by western blotting using antisera against Sox10 (1:1000 dilution) and Gapdh (1:3000 dilution, Santa Cruz Biotechnology), protein A coupled to horseradish peroxidase (Bio-Rad) and Luminol reagent for chemiluminescent detection.

Quantification and statistical analysis

For quantification of cell numbers, areas and g ratios, at least three spinal cord, brain or nerve sections from independent embryos or mice of each genotype were counted. All statistical analysis was performed with Prism6 software (GraphPad) or Excel 2016 (Microsoft Office). Statistically significant differences were determined by Student's *t* test.

Acknowledgements

We thank M. Schimmel for excellent technical assistance with electron microscopy.

Conflict of Interest statement. None declared.

Funding

This work was supported by a grant from the 'Cyder' emerging field initiative of Friedrich-Alexander Universität Erlangen-Nürnberg and the Interdisziplinäres Zentrum für klinische Forschung Erlangen to M.W. (D24).

References

1. Kelsh, R.N. (2006) Sorting out Sox10 functions in neural crest development. *Bioessays*, **28**, 788–798.
2. Inoue, K., Khajavi, M., Ohyama, T., Hirabayashi, S.-I., Wilson, J., Reggin, J.D., Mancias, P., Butler, I.J., Wilkinson, M.F., Wegner, M. *et al.* (2004) Molecular mechanism for distinct neurological phenotypes conveyed by allelic truncating mutations. *Nat. Genet.*, **36**, 361–369.
3. Pingault, V., Bondurand, N., Kuhlbrodt, K., Goerich, D.E., Prehu, M.-O., Puliti, A., Herbarth, B., Hermans-Borgmeyer, I., Legius, E., Matthijs, G. *et al.* (1998) Sox10 mutations in patients with Waardenburg-Hirschsprung disease. *Nat. Genet.*, **18**, 171–173.
4. Southard-Smith, E.M., Angrist, M., Ellison, J.S., Agarwala, R., Baxevanis, A.D., Chakravarti, A. and Pavan, W.J. (1999) The Sox10(Dom) mouse: modeling the genetic variation of Waardenburg-Shah (WS4) syndrome. *Genome Res.*, **9**, 215–225.
5. Pingault, V., Bodereau, V., Baral, V., Marcos, S., Watanabe, Y., Chaoui, A., Fouveaut, C., Leroy, C., Verier-Mine, O., Francannet, C. *et al.* (2013) Loss-of-function mutations in SOX10 cause Kallmann syndrome with deafness. *Am. J. Hum. Genet.*, **92**, 707–724.
6. Pingault, V., Bondurand, N., Le Caignec, C., Tardieu, S., Lemort, N., Dubourg, O., Le Guern, E., Goossens, M. and Boespflug-Tanguy, O. (2001) The SOX10 transcription factor: evaluation as a candidate gene for central and peripheral hereditary myelin disorders. The clinical E.N.B.D.D. clinical European network on brain dysmyelinating disease. *J. Neurol.*, **248**, 496–499.
7. Pingault, V., Ente, D., Dastot-Le Moal, F., Goossens, M., Marlin, S. and Bondurand, N. (2010) Review and update of mutations causing Waardenburg Syndrome. *Hum. Mutat.*, **31**, 391–406.
8. Chaoui, A., Kavo, A., Baral, V., Watanabe, Y., Lecerf, L., Colley, A., Mendoza-Londono, R., Pingault, V. and Bondurand, N. (2015) Subnuclear re-localization of SOX10 and p54NRB correlates with a unique neurological phenotype associated with SOX10 missense mutations. *Hum. Mol. Genet.*, **24**, 4933–4947.
9. Britsch, S., Goerich, D.E., Riethmacher, D., Peirano, R.I., Rossner, M., Nave, K.A., Birchmeier, C. and Wegner, M. (2001) The transcription factor Sox10 is a key regulator of peripheral glial development. *Genes Dev.*, **15**, 66–78.
10. Herbarth, B., Pingault, V., Bondurand, N., Kuhlbrodt, K., Hermans-Borgmeyer, I., Puliti, A., Lemort, N., Goossens, M. and Wegner, M. (1998) Mutation of the Sry-related Sox10 gene in *Dominant megacolon*, a mouse model for human Hirschsprung disease. *Proc. Natl. Acad. Sci. U. S. A.*, **95**, 5161–5165.
11. Southard-Smith, E.M., Kos, L. and Pavan, W.J. (1998) Sox10 mutation disrupts neural crest development in *Dom* Hirschsprung mouse model. *Nat. Genet.*, **18**, 60–64.
12. Stolt, C.C., Rehberg, S., Ader, M., Lommes, P., Riethmacher, D., Schachner, M., Bartsch, U. and Wegner, M. (2002) Terminal differentiation of myelin-forming oligodendrocytes depends on the transcription factor Sox10. *Genes Dev.*, **16**, 165–170.
13. Barraud, P., St John, J.A., Stolt, C.C., Wegner, M. and Baker, C.V. (2013) Olfactory ensheathing glia are required for embryonic olfactory axon targeting and the migration of gonadotropin-releasing hormone neurons. *Biol. Open*, **2**, 750–759.
14. Dutton, K.A., Pauliny, A., Lopes, S.S., Elworthy, S., Carney, T.J., Rauch, J., Geisler, R., Haffter, P. and Kelsh, R.N. (2001) Zebrafish colourless encodes sox10 and specifies non-ectomesenchymal neural crest fates. *Development*, **128**, 4113–4125.
15. Ito, Y., Inoue, N., Inoue, Y.U., Nakamura, S., Matsuda, Y., Inagaki, M., Ohkubo, T., Asami, J., Terakawa, Y.W., Kohsaka, S. *et al.* (2015) Additive dominant effect of a SOX10 mutation underlies a complex phenotype of PCWH. *Neurobiol. Dis.*, **80**, 1–14.
16. Inoue, K., Ohyama, T., Sakuragi, Y., Li-Hua, Y., Yamamoto, R., Yu, L.-H., Goto, Y.-I., Wegner, M. and Lupski, J. (2007) Translation of SOX10 3' untranslated region causes a complex severe neurocristopathy by generation of a deleterious functional domain. *Hum. Mol. Genet.*, **16**, 3037–3046.
17. Schreiner, S., Cossais, F., Fischer, K., Scholz, S., Bösl, M.R., Holtmann, B., Sendtner, M. and Wegner, M. (2007) Hypomorphic Sox10 alleles reveal novel protein functions and unravel developmental differences in glial lineages. *Development*, **134**, 3271–3281.

18. Finzsch, M., Schreiner, S., Kichko, T., Reeh, P., Tamm, E.R., Bösl, M.R., Meijer, D. and Wegner, M. (2010) Sox10 is required for Schwann cell identity and progression beyond the immature Schwann cell stage. *J. Cell. Biol.*, **189**, 701–712.
19. Maka, M., Stolt, C.C. and Wegner, M. (2005) Identification of Sox8 as a modifier gene in a mouse model of Hirschsprung disease reveals underlying molecular defect. *Dev. Biol.*, **277**, 155–169.
20. Hornig, J., Fröb, F., Vogl, M.R., Hermans-Borgmeyer, I., Tamm, E.R., Wegner, M. and Barres, B.A. (2013) The transcription factors Sox10 and Myrf define an essential regulatory network module in differentiating oligodendrocytes. *PLoS Genet.*, **9**, e1003907.
21. Kuhlbrodt, K., Herbarth, B., Sock, E., Hermans-Borgmeyer, I. and Wegner, M. (1998) Sox10, a novel transcriptional modulator in glial cells. *J. Neurosci.*, **18**, 237–250.
22. Stolt, C.C., Lommes, P., Friedrich, R.P. and Wegner, M. (2004) Transcription factors Sox8 and Sox10 perform non-equivalent roles during oligodendrocyte development despite functional redundancy. *Development*, **131**, 2349–2358.
23. Reiprich, S., Kriesch, J., Schreiner, S. and Wegner, M. (2010) Activation of Krox20 gene expression by Sox10 in myelinating Schwann cells. *J. Neurochem.*, **112**, 744–754.
24. Peirano, R.I. and Wegner, M. (2000) The glial transcription factor Sox10 binds to DNA both as monomer and dimer with different functional consequences. *Nucleic Acids Res.*, **28**, 3047–3055.
25. Schlierf, B., Ludwig, A., Klenovsek, K. and Wegner, M. (2002) Cooperative binding of Sox10 to DNA: requirements and consequences. *Nucleic Acids Res.*, **30**, 5509–5516.
26. Cossais, F., Wahlbuhl, M., Kriesch, J. and Wegner, M. (2010) SOX10 structure-function analysis in the chicken neural tube reveals important insights into its role in human neurocristopathies. *Hum. Mol. Genet.*, **19**, 2409–2420.
27. Kim, J., Lo, L., Dormand, E. and Anderson, D.J. (2003) SOX10 maintains multipotency and inhibits neuronal differentiation of neural crest stem cells. *Neuron*, **38**, 17–31.
28. Cantrell, V.A., Owens, S.E., Chandler, R.L., Airey, D.C., Bradley, K.M., Smith, J.R. and Southard-Smith, E.M. (2004) Interactions between Sox10 and EdnrB modulate penetrance and severity of aganglionosis in the Sox10Dom mouse model of Hirschsprung disease. *Hum. Mol. Genet.*, **13**, 2289–2301.
29. Walters, L.C., Cantrell, V.A., Weller, K.P., Mosher, J.T. and Southard-Smith, E.M. (2010) Genetic background impacts developmental potential of enteric neural crest-derived progenitors in the Sox10Dom model of Hirschsprung disease. *Hum. Mol. Genet.*, **19**, 4353–4372.
30. Kellerer, S., Schreiner, S., Stolt, C.C., Bösl, M.R. and Wegner, M. (2006) Replacement of the Sox10 transcription factor by Sox8 reveals incomplete functional equivalence. *Development*, **133**, 2875–2886.
31. Stolt, C.C., Lommes, P., Sock, E., Chaboissier, M.-C., Schedl, A. and Wegner, M. (2003) The Sox9 transcription factor determines glial fate choice in the developing spinal cord. *Genes Dev.*, **17**, 1677–1689.
32. Stolt, C.C., Schmitt, S., Lommes, P., Sock, E. and Wegner, M. (2005) Impact of transcription factor Sox8 on oligodendrocyte specification in the mouse embryonic spinal cord. *Dev. Biol.*, **281**, 323–331.
33. Friedrich, R., Schlierf, B., Tamm, E.R., Bösl, M.R. and Wegner, M. (2005) The class III POU domain protein Brn-1 can fully replace the related Oct-6 during Schwann cell development and myelination. *Mol. Cell. Biol.*, **25**, 1821–1829.
34. Peirano, R.I., Goerich, D.E., Riethmacher, D. and Wegner, M. (2000) Protein zero expression is regulated by the glial transcription factor Sox10. *Mol. Cell. Biol.*, **20**, 3198–3209.